

MIT Open Access Articles

Electron temperature fluctuations associated with the weakly coherent mode in the edge of I-mode plasmas

The MIT Faculty has made this article openly available. **Please share** how this access benefits you. Your story matters.

Citation: White, A.E., P. Phillips, D.G. Whyte, A.E. Hubbard, C. Sung, J.W. Hughes, A. Dominguez, J. Terry, and I. Cziegler. "Electron temperature fluctuations associated with the weakly coherent mode in the edge of I-mode plasmas." Nuclear Fusion 51, no. 11 (November 1, 2011): 113005.

As Published: <http://dx.doi.org/10.1088/0029-5515/51/11/113005>

Publisher: IOP Publishing

Persistent URL: <http://hdl.handle.net/1721.1/81467>

Version: Author's final manuscript: final author's manuscript post peer review, without publisher's formatting or copy editing

Terms of use: Creative Commons Attribution-Noncommercial-Share Alike 3.0



PSFC/JA-11-36

**Electron Temperature Fluctuations Associated with
the Weakly Coherent Mode in the Edge
of I-mode Plasmas**

White, A.E., Phillips, P*., Whyte, D.G., Hubbard, A.E., Sung, C.,
Hughes, J.W., Dominguez, Terry, J., Cziegler, I.

* University of Texas, Austin

January, 2012

**Plasma Science and Fusion Center
Massachusetts Institute of Technology
Cambridge MA 02139 USA**

This work was supported by the U.S. Department of Energy, Grant No. DE-FC02-99ER54512-CMOD. Reproduction, translation, publication, use and disposal, in whole or in part, by or for the United States government is permitted.

Electron Temperature Fluctuations Associated with the Weakly Coherent Mode in the Edge of I-mode Plasmas

A. E. White¹, P. Phillips², D. G. Whyte¹, A. E. Hubbard¹,
C. Sung¹, J. W. Hughes¹, A. Dominguez¹, J. Terry¹, I. Cziegler¹

¹ Massachusetts Institute of Technology, USA

² University of Texas - Austin, USA

E-mail: whitea@mit.edu

Abstract.

New measurements of electron temperature fluctuations associated with the weakly coherent mode (WCM) during improved mode, or I-mode plasmas [D. G. Whyte et al. Nucl. Fus. 50, 105005 (2010)] at Alcator C-Mod [E.S. Marmor et al., Fus. Sci. Tech. 51, 3261 (2007)] are presented in this paper. The measurements are made with a 32-channel, high-resolution profile ECE radiometer. The WCM electron temperature fluctuations are localized to a 1 cm region inside the last closed flux surface. The WCM electron temperature fluctuation level is measured in several different I-mode discharges and is in the range $1\% < \tilde{T}_e/T_e < 2\%$, which is an order of magnitude smaller than the WCM density fluctuation level. The WCM edge fluctuations observed in I-mode are believed to play a role in increasing particle transport but not energy transport in the edge of I-mode plasmas. The large difference between normalized density and electron temperature fluctuation amplitudes provides new evidence that the WCM fluctuations can separately affect energy and particle transport.

1. Introduction

The improved mode, or I-mode, regime of operation [1, 2] on Alcator C-Mod [4] is characterized by the presence of an edge thermal transport barrier and the absence of an edge particle transport barrier. I-mode, an operating regime distinct from L-mode and H-mode, allows for high confinement and high pressure but without ELMs and without impurity accumulation, which makes I-mode of interest for burning plasma regimes. During I-mode, there is a reduction in low frequency ($f < 100$ kHz) edge fluctuations compared to L-mode as well as the presence of the weakly coherent mode (WCM) oscillation with center frequency $150 < f_0 < 250$ kHz, and bandwidth $\Delta f \approx 100$ kHz. These unique edge turbulence characteristics are observed only during I-mode and are identified in the autopower spectrum of density fluctuations measured with reflectometer and Gas Puff Imaging (GPI) diagnostics, as well as in the autopower spectrum of edge magnetic probe signals [1, 2]. The WCM has density fluctuation levels in the range of $\tilde{n}/n = 6\text{--}13\%$, which is at least $10 - 15\%$ above L-mode fluctuation levels [2, 3]. The WCM is localized to a 1-2 cm region inside the last closed flux surface (LCFS), and propagates in the electron diamagnetic drift direction [1, 2].

Because I-mode exhibits significant particle transport, with suppressed energy transport [1], it has been speculated that the edge-localized, WCM electromagnetic fluctuations play a role in increasing particle transport and regulating the edge pressure in I-mode [1, 2]. It is important to characterize the amplitudes of fluctuating electrostatic potential, magnetic field, density and temperature (and the cross-phases between these fluctuating fields) in order to determine the possible drive mechanisms for the WCM and the effects on particle and energy transport. While density, temperature and magnetic fluctuations can all contribute to thermal transport, particle transport due to electromagnetic drift-wave instabilities is typically associated with density and magnetic fluctuations [5, 6, 7].

During I-mode, the presence of the WCM correlates with reduced thermal transport, with no accompanying reduction in particle transport. If the WCM is a typical drift-wave type instability with both density and temperature fluctuations associated with it, and these fluctuations are in phase with the potential fluctuations of the WCM so that they both contribute to transport (e.g. see Eqns. 4 and 7 of Ref. [7]), then the separation between the two transport channels could be explained, at least in part, if the temperature fluctuation amplitude of the WCM were lower than the density fluctuation amplitude of the WCM. This is because both density and temperature fluctuations can drive the thermal transport, but only the density fluctuations drive the particle transport. There is a proposed drift-wave type instability that could explain the WCM - the heavy particle mode [9, 10, 11, 12]. The heavy particle mode driving the observed WCM would be consistent with the presence of significant density fluctuations and relatively weak or negligible temperature fluctuations.

The previous studies of the WCM in I-mode at Alcator C-Mod pointed out the critical need to quantify the temperature fluctuations, but no measurements of

temperature fluctuations were available. Since these experiments, the 32-channel high resolution Electron Cyclotron Emission (ECE) profile radiometer [8] at Alcator C-Mod has been upgraded to allow for new, detailed measurements of the WCM. Temperature fluctuations associated with the WCM have been clearly observed in the autopower spectrum, cross-spectrum and coherency spectrum of fast-sampled ECE radiometer signals.

In this paper, we present the first measurements of electron temperature fluctuations associated with the weakly coherent mode (WCM) in the edge of I-mode plasmas. The measurements show that the electron temperature fluctuation amplitude associated with the WCM is in the range $1\% < \tilde{T}_e/T_e < 2\%$. During L-mode, only an upper limit can be placed on the fluctuation level in the same frequency range, $(\tilde{T}_e/T_e)_{upper} < 0.5\%$, which indicates that the I-mode WCM electron temperature fluctuation level is at least a factor of two above L-mode fluctuation levels. The ECE radiometer measurements show that the WCM is highly localized to a narrow < 1 cm region inside the LCFS, consistent with measurements of WCM density fluctuations with reflectometer and GPI [2]. Quantitative measurements of electron temperature fluctuations associated with WCM are important for guiding modeling and theory for the WCM, and for planning future experiments at C-Mod and other tokamaks. Measuring the electron temperature fluctuations is also important for identifying the underlying instability responsible for the observed WCM fluctuations.

2. Experimental Set-Up

2.1. High resolution radiometer

The 32-channel radiometer at Alcator C-mod [8] is used to measure the electron temperature fluctuations associated with the WCM. The radiometer is measuring the radiation temperature, T_{rad} , of the 2nd harmonic electron cyclotron emission (ECE) [13]. When detecting optically thick ECE on the low field side of the tokamak with the angle of view roughly perpendicular to the total magnetic field direction, the measured radiation temperature, T_{rad} , can be confidently identified as the electron temperature T_e . Because of the $1/R$ dependence of the magnetic field in a tokamak, $B(R) \approx B_o R_o/R$, where R is the major radius, B_o is the field on axis at $R_o = R$, the frequency of cyclotron emission also varies with $1/R$ and there is a direct relation between frequency resolved measurements of the intensity and the radial location of emission.

The spatial resolution of the radiometer has been described in detail previously [8, 14, 15]. Poloidal resolution is determined by the focusing optics, which produce a spot-size in the plasma of roughly 3 cm. Because the system views the plasma at an angle of 20° degrees below the midplane [15], radial resolution is limited by the overlap of the poloidal spot-size onto neighboring flux surfaces, but also depends on a combination of the intermediate frequency (IF) filter bandwidth and relativistic line broadening. These effects result in radial resolution of $\Delta R \leq 1$ cm in the edge plasma. Corresponding

wavenumber sensitivity to fluctuations is $k_\theta < 5.1 \text{ cm}^{-1}$ and $k_x < 5.6 \text{ cm}^{-1}$, where x denotes the direction of line-of-sight of the radiometer. The radial location for a T_e measurement is selected by the center frequency of the IF filter, and in the present system the IF filters sample disjoint frequency bands, separated center-to-center by 2.2 GHz. The bandwidth of the IF filters is $B_{IF} = 1.5 \text{ GHz}$, the video bandwidth is $B_{VID} = 1 \text{ MHz}$ [8], and the signals are digitized at 2 MHz. In much of the data examined here, there are narrow ($\Delta f < 3 \text{ kHz}$) noise peaks present in the radiometer signals. This electronics noise is not a plasma effect and is correlated across all radiometer channels. These noise peaks can be filtered out and do not inhibit the measurement of the WCM fluctuation spectrum or measurements of the electron temperature fluctuation level.

A single ECE radiometer channel will be sensitive to narrowband fluctuations ($B_{sig} < B_{VID}$) that are above the level $\delta T/T = \sqrt{B_{sig}/B_{IF}}$, where B_{sig} is the bandwidth of the signal [16]. In the case of I-mode measurements of the WCM the full width at half maximum (FWHM) frequency width of the mode has been reported to be between 50 – 100 kHz [1]. The video bandwidth of the radiometer is set by hardware at a maximum of 1 MHz. This means that for the Alcator C-Mod radiometer it is true that $B_{sig} < B_{VID}$ and a single ECE radiometer channel should be sensitive to WCM electron temperature fluctuations as long as $\delta T/T \geq 0.7 - 1.0\%$, with this sensitivity limit depending on the FWHM of the fluctuation spectrum.

With correlation ECE techniques, if two radiometer measurements are made in disjoint frequency bands, but within the correlation length of the turbulence, then the thermal noise is suppressed and the temperature fluctuations below the inherent thermal noise sensitivity limit can be measured [17]. When the WCM cannot be directly observed in the autopower spectrum, it can be observed with the cross-correlation, the cross-power and the coherency spectrum calculated between neighboring radiometer channels. But in contrast to typical correlation ECE measurements [18, 19], for the radiometer used here it is not true the temperature and temperature fluctuations measured on two channels are the same, because the channels are not always sampling the same emission layer due to the center frequency differences between IF filters. When applying correlation ECE analysis to two radiometer signals, S_1 and S_2 , that do originate from the same emission layer, the fluctuation level can be calculated from the cross-correlation coefficient, $C_{1,2}$, or the cross-covariance, $R_{1,2}$ at zero time delay, or by integrating the cross-power spectrum [20, 19, 16]. When the cross-correlation methods are applied to the C-Mod radiometer, we are strictly calculating the product of the relative fluctuation levels of the two signals, e.g. $\langle S_1 S_2 \rangle \approx (\tilde{T}_1/T_1)(\tilde{T}_2/T_2)$. From the covariance, $R_{xy}(\tau = 0)$ or from the integrated cross-power spectrum we can measure $(\tilde{T}_1/T_1)(\tilde{T}_2/T_2)$. Obtaining fluctuation levels from the covariance, cross-power spectrum or autopower spectrum requires calibration of the radiometer. It is also possible with correlation ECE analysis to measure fluctuation levels without needing the radiometer calibration by using cross-correlation coefficient, $C_{1,2}(\tau = 0)$. In this case, $(2B_{vid}/B_{if})C_{1,2}(\tau = 0) = (\tilde{T}_1/T_1)(\tilde{T}_2/T_2)$. The autopower spectrum, cross-power spectrum, coherency spectrum, covariance and cross-correlation coefficient are all calculated here using standard definitions and techniques

[21].

2.2. Edge temperature measurements with ECE radiometry

ECE radiometers are standard tokamak diagnostics capable of measuring radial profiles of electron temperature with excellent spatial and temporal resolution. However, the interpretation of the radiometer signal intensity as electron temperature in the edge and pedestal region is typically limited by low optical depth. The optical depth for the second harmonic X-mode ECE is given as [22]

$$\tau_2^x = \frac{2\pi^2 R_o \omega_{pe}^2}{\lambda_0 \omega_{ce}^2} \left(\frac{kT_e}{m_e c^2} \right) \quad (1)$$

where $\lambda_0 = 2\pi c/\omega_{ce}$ and R_o is the major radius of the tokamak. If this limitation is carefully considered, then radiometer measurements of electron temperature and temperature fluctuations can be extended to the edge of the plasma. We note that limits on the use of ECE radiometers to measure edge pedestal temperatures have been previously quantified [23, 24] and recently ECE radiometers have been used to make detailed measurements of low-field-side and high-field-side pedestal temperatures on the JET tokamak [25]. In Alcator C-Mod it is typically the case in I-mode plasmas that the optical depth is high enough even in the far edge region that an ECE signal can be taken as a direct measurement of electron temperature. For optical depth $1.5 < \tau < 3$ the single-pass emission can be below the blackbody level, but the effect of wall reflections and multiple-passes increases the intensity to the blackbody level. For this optical depth range, it has been shown that T_e can be obtained rather directly from the ECE measurements without needing a detailed model of the effects of wall reflections [23]. If $0.6 < \tau < 1.5$, detailed models of the effects of wall reflections are needed to recover T_e from the measured ECE, and for $\tau < 0.6$ measurements of T_e are not possible. Comparisons with the high resolution edge Thomson Scattering system [26] on C-Mod provides the capability to cross-check the edge ECE radiometer measurements of T_e , and the two measurements are in good agreement for the plasmas considered here (e.g. Figure 1).

If the optical depth is sufficiently high, the radiometer can also be used as an edge fluctuation diagnostic, which can provide key information about the spectrum and amplitude of edge electron temperature perturbations. ECE radiometers have been successfully employed in the edge of tokamaks where the optical depth is low to measure temperature perturbations associated with ELMs [23, 27]. When measuring fluctuations, the limits placed on the optical depth are more stringent in order to avoid contributions from density fluctuations to the measured signal. One contribution occurs due to density fluctuations modulating the optical depth, which results in apparent temperature fluctuations in the measured EC emission [28]. This effect on measurements of temperature fluctuations with radiometers in plasmas that are marginally optically thick has been modeled previously [28, 29, 30] and it can be shown that when $\tau > 3 - 4$ estimated effects of even large ($> 10\%$) density fluctuations are

typically negligible. Various other mechanisms give rise to additional contributions to the measured temperature fluctuations due to both density and magnetic fluctuations and these effects have been discussed and modeled [30]. We note that without detailed information on the density fluctuation amplitude, local magnetic field fluctuation amplitude, and the phases between the fluctuating fields, the estimates are used only to provide an upper limit on contributions from density and magnetic field fluctuations to the measured radiation temperature fluctuations.

3. Experimental Results

3.1. I-mode plasma parameters

I-mode plasmas at Alcator C-Mod are characterized by steep edge pedestals in temperature, but not in density. In I-mode the normalized energy confinement and stored energy are comparable to H-mode plasmas at Alcator C-Mod and steady I-modes (> 10 confinement times) are regularly achieved at C-Mod [2] and have been studied across a wide range of parameters ($3 < B_t < 6$ T, $0.7 < I_p < 1.3$ MA, $0.86 \leq \langle n_e \rangle \leq 2.05 \times 10^{20}$ m $^{-3}$). In this work, several I-mode shots that exhibited clear WCM fluctuations are examined. Plasma parameters are shown for a representative I-mode shot (1101209012) in Fig. 1 with toroidal field, $B_T = 5.7$ T, plasma current, $I_p = 1.1$ MA, edge safety factor $q_{95} = 3.8$, with 3.1 MW of ion cyclotron resonance heating (ICRH) power. Figure 1 shows the input RF-power and the increase in core temperature, edge temperature, and stored energy that occur during the I-mode phase ($0.7 < t < 1.5$ sec) of the discharge. Across the L-I transition ($t_{LI} \approx 0.75$ sec), there is little to no change in line averaged density and local edge density. The I-mode transition is identified by the significant increases in core temperature, edge temperature, and stored energy and also by the appearance of the WCM in the edge plasma. During the I-mode phase between $t = 0.8$ – 1.5 sec the line averaged density is $\langle n_e \rangle = 1.25 \times 10^{20}$ m $^{-3}$, the central density is $n_e(0) = 2.14 \times 10^{20}$ m $^{-3}$, and the central temperature is $T_e(0) \approx 4.0$ keV. Later in the shot when the RF power is turned off, the plasma transitions back into L-mode. As shown in Fig. 2, the density profiles during I-mode and L-mode are similar, but during I-mode there is a large increase in edge temperature and a steep electron temperature gradient. Edge Thomson Scattering and ECE data from a Grating Polychrometer diagnostic are fit with a modified tanh function [31]. The fits to the edge profiles are used to calculate the profiles of the optical depth in the edge region. In Fig. 2, (a) profiles of edge electron temperature and (b) density are shown for the L-mode (black-triangles) phase and the I-mode phase (red-asterisk) of discharge 1101209012. Shown in Fig. 2 (c), the optical depth in I-mode (red) just ~ 5 mm inside the LCFS is $\tau \geq 4$, which is significantly higher than L-mode (black) where $\tau \approx 1$ at the same radial location.

Using magnetics-constrained EFIT equilibrium reconstruction, the edge radiometer measurement locations are mapped to the midplane. For these plasmas, after mapping to

the midplane, the typical measurement locations are as follows: channel 2 ($f_{ece} = 237.3$ GHz) is at $R = 90.9$ cm, $r/a = 1.07$; channel 3 ($f_{ece} = 239.6$ GHz) is at $R = 90.1$ cm, $r/a = 1.02$; channel 4 ($f_{ece} = 241.8$ GHz) is at $R = 89.4$ cm, $r/a = 0.98$; channel 5 ($f_{ece} = 244.1$ GHz) is at $R = 88.7$ cm, $r/a = 0.93$; where the minor radius $a = 22$ cm. An ECE measurement location for a fixed frequency depends only on total magnetic field and is constant during the entire current flattop and during the I-mode phase of interest.

In all shots considered here and at all times of interest the optical depth at the radiometer channel 4 measurement locations has $\tau \geq 2$. The WCM is radially localized to the region of the plasma where gradients in density and temperature are large and τ can vary significantly within the narrow 1 cm region inside the LCFS where the WCM is observed. The error in the optical depth is estimated at 20% and is dominated by the random error in the measured temperature and density profiles.

3.2. Spectral Features of the WCM

The WCM fluctuations during I-mode are clearly seen in shot 1101209012. The contour autopower spectra plotted versus frequency and time for edge ECE radiometer, reflectometer and magnetics signals are shown in Fig. 3. The transition from L-mode to I-mode occurs at $t \approx 0.7$ sec. A transition back into L-mode occurs at $t \approx 1.4$ sec after RF power is turned off. The WCM is clearly seen during the long I-mode phase of the shot in the autopower spectra of magnetics signals (a), a reflectometer signal at $R = 89.6$ cm (b), and a radiometer signal at $R = 89.4$ cm (c). The WCM spectral features in magnetic, density, electron temperature fluctuations are similar. The WCM has center frequency $f_{center} \approx 220$ kHz and $\delta f_{FWHM} \approx 50$ kHz during the long I-mode phase. Figure 3 (d) shows the temperature fluctuation amplitude as a function of time, measured with the radiometer signal shown in Fig. 3 (c). The fluctuation level is calculated using a 50 ms sliding time average, and the data points shown correspond to the center of the time window. The red dashed line indicates the radiometer sensitivity limit in this case. During L-mode, $t < 0.7$ s and $t > 1.4$ s, the temperature fluctuations, either of a broadband nature or limited to the WCM frequency band, cannot be resolved. This lack of measured fluctuations in L-mode is most likely due to the sensitivity limit of the radiometer. A detailed description of how the fluctuation amplitude is calculated is given in Section 3.4.

As seen in Figure 3 (c), the temperature fluctuation spectral has $\delta f_{FWHM} \approx 50$ kHz for the WCM in this case. Then the temperature fluctuations must have amplitude $\delta T/T \geq 0.7\%$ during I-mode to be detected. Based on reflectometer measurements during L-mode, the spectrum of edge fluctuations is much broader than the WCM in I-mode. If we take the $\delta f_{FWHM} \approx 250$ kHz during L-mode, then temperature fluctuations must have amplitude $\delta T/T \geq 1.6\%$ during L-mode to be detected. This indicates that broadband edge temperature fluctuations during L-mode are at least a factor of two lower in amplitude than the WCM temperature fluctuations during I-

mode. One caveat is that we have assumed the spectral shape of the temperature fluctuations during L-mode is the same as the density fluctuation spectrum, which may not be true. One consequence of the sensitivity limit is that the reduction of low-frequency fluctuations accompanying the emergence of the WCM that is observed with reflectometer measurements cannot be assessed in this work with the available radiometer measurements. Measurements of temperature fluctuations during L-mode, and measurements of the temperature fluctuation spectral evolution across the L-I-mode transition, will require the use of a dedicated correlation ECE radiometer [17, 18, 19], which is currently planned for C-Mod [32].

3.3. Radial Localization of the WCM

Another consequence of the sensitivity limits (Section 2.1) is that the WCM cannot always be observed in the autopower spectrum of a single radiometer channel. That is, if $\delta f_{FWHM} \approx 50$ kHz for the WCM and temperature fluctuations have $\delta T/T < 0.7\%$, then the WCM temperature fluctuation amplitude is below the thermal-noise limited sensitivity of a single channel. In these case, the WCM temperature fluctuation spectrum can often still be observed using the correlation ECE technique [17, 18, 19]. As shown in Fig. 4 (a), the WCM is seen clearly in the autopower spectrum of one edge ECE channel, but the WCM is not seen in the power spectrum of a neighboring channel (b). These spectra are ensemble averages, calculated between $t = 0.85 - 1.15$ sec. The coherency between these two ECE channels is shown in Fig. 4 (c). The coherency peaks at $\gamma = 0.3$ at $f = 200$ kHz. In other similar shots, coherency as high as 0.5 has been measured between edge ECE channels during I-mode.

The WCM is never correlated on more than two radiometer channels, and it is always correlated between the two channels that are just at the LCFS and roughly 0.5 cm inside the plasma. The WCM is not observed to be correlated on any other radiometer channels further inside the LCFS. The ECE sample volumes for the radiometer channels in the edge do slightly overlap due to the curvature of the flux surfaces and the off-midplane viewing angle of the ECE radiometer [8]. Based on reflectometer and Gas Puff Imaging measurements of density fluctuations, the radial localization of the WCM has been reported to extend from roughly 1 cm inside the LCFS to the LCFS [1, 2]. The radial structure of the WCM temperature fluctuations observed with the radiometer is consistent with these past observations. In this particular shot, 1101209012, during I-mode the WCM is correlated between channels 3 and 4, but not between channels 2 and 3 or between channels 4 and 5 (or any other channels that are deeper in the plasma).

3.4. Electron Temperature Fluctuation Amplitude of the WCM

The radiometer channels are calibrated and the relative fluctuation level can be calculated from the time-averaged autopower spectrum of a radiometer signal, Fig. 4 (a). The spectrum is first integrated between $50 < f < 300$ kHz, where the WCM is observed. The background thermal noise levels, which are approximated by integrating

Table 1. Summary of fluctuation amplitude analyses. The autopower spectrum integrated between 50 – 350 kHz is used to calculate the fluctuation level. The radial locations, local values of T_e , n_e , and optical depth, τ , are listed. Also given is the major radius of the LCFS.

Shot	Time (sec)	\tilde{T}_e/T_e (%)	R_{maj} (cm)	R_{LCFS} (cm)	r/a –	T_e (eV) (eV)	n_e (10^{20} m $^{-3}$) (10^{20} m $^{-3}$)	τ –
1101209010	0.8-1.4	1.56%	89.3	89.6	0.98	300	1.3	3.0
1101209011	0.8-1.2	1.59%	89.3	89.6	0.98	350	1.3	3.6
1101209012	0.8-1.4	1.37 %	89.3	89.6	0.97	350	1.4	3.8
1101209013	0.8-1.3	1.42 %	89.4	89.6	0.99	400	1.3	4.1
1101209031	1.2-1.4	1.11 %	89.5	89.9	0.97	200	1.3	2.0

the ECE power spectrum in a neighboring frequency band where the WCM is not present, $350 < f < 600$ kHz, are subtracted to obtain the measured fluctuation level. For channel 4 between $0.85 < t < 1.25$ sec (1101209013), when the mode is seen strongly in the autopower spectrum, the fluctuation level is $\tilde{T}_e/T_e(r/a = 0.98) = 1.44\%$, which is above the single channel sensitivity limit, $\approx 0.7\%$. For the same shot and time, the fluctuation level between $50 < f < 300$ kHz for channel 3 (Fig. 4 (b)) is equivalent to the integrated thermal noise level ($350 < f < 600$ kHz). The optical depth at these two locations is $\tau \approx 4$ and $\tau \approx 1$, respectively.

The WCM density fluctuation amplitude (relative to L-mode) is roughly a factor of three lower than the Quasi-Coherent Mode (QCM) amplitude (relative to L-mode) [2]. The density fluctuation amplitude of the QCM has been measured in the range $\tilde{n}/n = 30 - 50\%$ using Langmuir probes [33, 34]. If we take the QCM amplitude to be $\tilde{n}/n \approx 30 - 50\%$ then the amplitude of the WCM would be $\tilde{n}/n \approx 10 - 16\%$. Recent GPI measurements have found WCM relative density fluctuation levels in the range of $\tilde{n}/n = 6?13\%$ [3], which is consistent with the estimated range based on comparisons with the measured QCM amplitude hubbard11. Our measurements indicate that the WCM temperature fluctuation level, \tilde{T}_e/T_e , can be up to an order of magnitude smaller than the WCM density fluctuation level, \tilde{n}/n .

For shot 1101209013, we correlate radiometer channels 4 and 3, averaged over $0.9 < t < 1.0$ sec, and find that $R_{xy}(\tau = 0) = (\tilde{T}_{e,4}/T_{e,4})(\tilde{T}_{e,3}/T_{e,3}) = 0.0117$, the integral of the cross-power spectrum between $50 < f < 300$ kHz gives $(\tilde{T}_{e,4}/T_{e,4})(\tilde{T}_{e,3}/T_{e,3}) = 0.0114$, and $2B_{vid}/B_{if}C_{xy}(\tau = 0) = (\tilde{T}_{e,4}/T_{e,4})(\tilde{T}_{e,3}/T_{e,3}) = 0.0111$. The value of $R_{xy}(\tau = 0)$ depends on the calibration of the radiometer, but the value of $(2B_{vid}/B_{if})C_{xy}(\tau = 0)$ does not. The good agreement between these two calculations confirms that there is no systematic or calibration error which could lead to a gross over-estimate or under-estimate of the fluctuation levels when using the autopower spectra. Using the measured fluctuation level from the autopower spectrum from channel 4, and the product of the fluctuation levels from the cross-power spectrum, an upper limit on the fluctuation level at the channel 3 radial location is inferred. For shot 1101209013, $0.9 < t < 1.0$

sec, we calculate $\tilde{T}_{e,4}/T_{e,4} = 1.6\%$ and $(\tilde{T}_{e,4}/T_{e,4})(\tilde{T}_{e,3}/T_{e,3}) = 0.0114$, which gives $\tilde{T}_{e,3}/T_{e,3} \approx 0.7\%$. Because of the lower optical depth at the channel 3 measurement location ($\tau \approx 1$), this value is only an upper limit on the temperature fluctuation level at that radius. This indicates that the WCM fluctuation amplitude peaks inside the last closed flux surface, where the optical depth is high, $\tau > 3$, and that there is a finite, but lower, fluctuation level nearer the LCFS.

3.5. Contributions from Density Fluctuations

For the ECE WCM measurement with channel 4 at $r/a \approx 0.98$ in shots 1101209010, 11, 12, and 13, the optical depth is large enough ($\tau > 3$) that density fluctuation contributions cannot account for the entire measured fluctuation amplitude [28, 29, 30]. In contrast, for measurements when the optical depth is $\tau \leq 2$, density fluctuations modulating the optical depth can potentially account for all of the measured fluctuation level. The contribution of density fluctuations to the measured electron temperature fluctuations can be modeled as modifications of the optical depth (at constant temperature) because τ_2^x is proportional to the product of density and electron temperature [29, 28]. The contribution of density fluctuations to measured temperature fluctuations is written as

$$\tilde{T}_m/T_m = [1 + C(\tau, \xi)] \frac{\tilde{T}_e}{T_e} + C(\tau, \xi) \frac{\tilde{n}_e}{n_e} \quad (2)$$

where \tilde{T}_m/T_m is the measured fluctuation amplitude, \tilde{T}_e/T_e is the electron temperature fluctuation amplitude, and \tilde{n}_e/n_e is the density fluctuation amplitude. Here

$$C(\tau, \xi) = \frac{\tau e^{-\tau}}{1 - e^{-\tau}} \left(1 - \xi \frac{1 - e^{-\tau}}{1 - \xi e^{-\tau}} \right) \quad (3)$$

where τ is the optical depth, and ξ is the wall reflectivity. It is not realistic to neglect the effects of wall reflections, as these have been shown to significantly enhance the ECE intensity from optically thin and marginally optically thick harmonics [13] and we take here $\xi = 0.85$.

This effect of density fluctuations on the radiometer signals depends very sensitively on the amplitude of the density fluctuations and the phase angle between density and electron temperature fluctuations. We assume that the electron temperature and density fluctuations are perfectly correlated, which means the contribution from density fluctuations is a maximum. We consider a range of WCM density fluctuation levels, $\tilde{n}/n = 5, 10, 15\%$ and 20% , when estimating the possible density fluctuation contributions to the radiometer measurements. Shown in Fig. 5, the measured fluctuation level, \tilde{T}_m/T_m is shown as the black, horizontal dashed line. The solid lines are the values of \tilde{T}_e/T_e calculated from (Eqn. 2) that correspond to the measured value for a given optical depth and given density fluctuation level. The differences between the measured value (horizontal dashed) and the calculated values (solid) lines are due to contributions from density fluctuations. Here we will call this estimated contribution from density fluctuations to the measured temperature fluctuation level an effective

temperature fluctuation, \tilde{T}_{eff}/T_{eff} . As shown in Fig. 5, the highest measured level of $\tilde{T}_m/T_m \approx 1.6\%$ is considered (see Table 1). With $\tau = 3.6$, density fluctuations contribute very little to the measured fluctuation level even if WCM $\tilde{n}/n = 20\%$ (blue), and the estimated upper bound contribution from density fluctuations modulating the optical depth is $\tilde{T}_{eff}/T_{eff} \approx 0.4\%$.

There are other possible ways that density fluctuations can affect the radiometer measurements. Another density fluctuation contribution can arise due to variations in the width of the emission layer due to modifications of the optical depth in a steep gradient region [30]. As the optical depth fluctuates, due to both density and temperature fluctuations, then the width of the emission layer will fluctuate, and the measurement volume is effectively being pushed back and forth across a temperature gradient, ∇T_e , as the extent of layer on the high field side of the resonance location varies. Additionally, the radiometer views the plasma from 20° degrees below the midplane [8] and this off-axis viewing angle makes the ECE radiometer signals sensitive to density fluctuations due to the effects of refraction [35]. Ray-tracing analysis can be used to assess quantitatively the impact of refraction, but these effects are not expected to be larger than the optical depth modulation effects already modeled here. Typically, even with a very large viewing angle as long as the local density in the ECE measurement region is $n_e < 0.85n_c$, where n_c is the cut-off density, refractive effects are negligible [36, 35]. We note that in 5.4T I-mode plasmas, $n_e \ll n_c$. Finally, electron temperature fluctuations can also arise from magnetic fluctuations giving rise to field line displacement, which move the ECE measurement volume across a temperature gradient [30]. Estimates of the magnetic fluctuation level of the WCM have been reported as $\frac{\delta B}{B} = 0.007 - 0.02\%$ [2] based on poloidal magnetic field probes located external to the plasma, but there are no measurements of magnetic field fluctuations in the edge plasma that could be used to model the effects of $\frac{\delta B}{B} = 0.007 - 0.02\%$ on the radiometer measurements. Future modeling work and measurements will be needed in order to investigate in more detail the possible contributions from magnetic field and density fluctuations to the measured temperature fluctuations.

4. Conclusions

New edge fluctuation measurements made with the upgraded high-resolution radiometer at Alcator C-Mod show that electron temperature fluctuations are associated with the weakly coherent mode (WCM) during I-mode confinement regimes. The WCM electron temperature fluctuations are localized to a narrow, ≤ 1 , cm radial region inside the LCFS. The measured normalized fluctuation levels are in the range $1\% < \tilde{T}_e/T_e < 2\%$. This is at least an order of magnitude smaller compared to the estimated WCM density fluctuation level [33, 34, 2]. The largest source of uncertainty in this result is the low optical depth in the edge region that introduces the possibility of large WCM density fluctuations contributing to the measured temperature fluctuation level [28, 29, 30]. We used here a model for the effects of optical depth modulation, which includes

the effects of wall reflections [28], in order to estimate possible contributions from density fluctuations to the measured temperature fluctuations. The model shows that the density fluctuations cannot account for the majority of the measured temperature fluctuations in the hot I-mode pedestal, even if $\tilde{n}/n = 20\%$ and the temperature and density fluctuations are perfectly in phase.

The measured electron temperature fluctuations associated with the WCM provide insight into how the WCM fluctuations might separately affect energy and particle transport during I-mode. For electromagnetic drift-wave turbulence, density, temperature and magnetic fluctuations can all contribute to thermal transport. But particle transport is only associated with density and magnetic fluctuations [5, 6, 7]. Given that the appearance of the WCM and associated density and magnetic fluctuations correlate with reduced thermal transport, with no accompanying reduction in particle transport, it is reasonable to expect that WCM temperature fluctuation amplitudes might be lower in I-mode relative to density fluctuations. A proposed drift-wave instability that could explain the WCM is the heavy particle mode [9, 10, 11, 12], which would have large density fluctuations compared to small, even negligible, electron temperature fluctuations.

Future work will include more detailed measurements of the WCM using the extensive suite of edge fluctuation diagnostics at Alcator C-Mod. In particular, Langmuir probe measurements of electron temperature fluctuations are possible in the edge plasma, and Gas Puff Imaging could also potentially be used to measure edge temperature fluctuations. These new measurements could be directly compared to the radiometer measurements. In future experiments, it will also be possible to correlate the measured magnetic fluctuations and density fluctuations with the measured temperature fluctuations. Determining if the density and temperature fluctuation levels peak at the same or slightly offset radial locations will require simultaneous measurements of localized density and temperature fluctuations, as can be performed with coupled radiometer and reflectometer diagnostics. Coupled radiometer and reflectometer diagnostics can also be used to measure the phase angle between density and electron temperature fluctuations [37], which will provide more information about the nature of the WCM and will also allow for better estimates of the density fluctuation contributions to the radiometer measurements.

Acknowledgments

The authors would like to thank Ron Parker for supporting the ECE radiometer digitizer upgrade, Josh Stillerman for helping with the digitizer set-up and testing, and the entire Alcator C-Mod team for their support of these measurements. This work supported by the US Department of Energy under DE-FC02-99ER54512-CMOD.

References

- [1] D.G. Whyte, A.E. Hubbard, J.W. Hughes, B. Lipschultz, J.E. Rice, E.S. Marmor, M. Greenwald, I. Cziegler, A. Dominguez, T. Golfopoulos, N. Howard, L. Lin, R.M. McDermott, M. Porkolab, M.L. Reinke, J. Terry, N.Tsujii, S. Wolfe, S. Wukitch, Y. Lin, and the Alcator C-Mod Team. I-mode: an H-mode energy confinement regime with I-mode particle transport in Alcator C-Mod. *Nuclear Fusion*, 50(10):105005, 2010.
- [2] A.E. Hubbard, D.G. Whyte, R.M. Churchill, I. Cziegler, A. Dominguez, T. Golfopoulos, J.W. Hughes, J.E. Rice, I. Bespamyatnov, M.J. Greenwald, N. Howard, B. Lipschultz, E.S. Marmor, M.L. Reinke, W.L. Rowan, J.L. Terry, and Alcator C-Mod Group. Edge energy transport barrier and turbulence in the I-mode regime at Alcator C-Mod. *Phys. Plasmas*, 18:056115, 2011
- [3] I. Cziegler. Turbulence and Transport Phenomena in Edge and SOL plasmas. *PhD Thesis*, MIT-PSFC, 2011
- [4] E. Marmor, A. Bader, M. Bakhtiari, H. Barnard, W. Beck, I. Bespamyatnov, A. Binus, P. Bonoli, B. Bose, M. Bitter, I. Cziegler, G. Dekow, A. Dominguez, B. Duval, E. Edlund, D. Ernst, M. Ferrara, C. Fiore, T. Fredian, A. Graf, R. Granetz, M. Greenwald, O. Grulke, D. Gwinn, S. Harrison, R. Harvey, T.C. Hender, J. Hosea, K. Hill, N. Howard, D.F. Howell, A. Hubbard, J.W. Hughes, I. Hutchinson, A. Ince-Cushman, J. Irby, V. Izzo, A. Kanojia, C. Kessel, J.S. Ko, P. Koert, B. LaBombard, C. Lau, L. Lin, Y. Lin, B. Lipschultz, J. Liptac, Y. Ma, K. Marr, M. May, R. McDermott, O. Meneghini, D. Mikkelsen, R. Ochoukov, R. Parker, C.K. Phillips, P. Phillips, Y. Podpaly, M. Porkolab, M. Reinke, J. Rice, W. Rowan, S. Scott, A. Schmidt, J. Sears, S. Shiraiwa, A. Sips, N. Smick, J. Snipes, J. Stillerman, Y. Takase, D. Terry, J. Terry, N. Tsujii, E. Valeo, R. Vieira, G. Wallace, D. Whyte, J.R. Wilson, S. Wolfe, G. Wright, J. Wright, S. Wukitch, G. Wurden, P. Xu, K. Zhurovich, J. Zaks, and S. Zweben. Overview of the Alcator C-Mod research program. *Nuclear Fusion*, 49(10):104014, 2009.
- [5] W. Horton. *Reviews of Modern Physics*, 71:735, 1999.
- [6] D. W. Ross. On standard forms for transport equations and quasilinear fluxes. *Plasma Phys. Control. Fusion*, 34:137, 1992.
- [7] A.J. Wootton, B.A. Carreras, H. Matsumoto, K. McGuire, W.A. Peebles, Ch.P. Ritz, P.W. Terry, S.J. Zweben. Fluctuations and anomalous transport in tokamaks. *Phys. Fluids B*, 2(12):2879, 1990.
- [8] J. W. Heard, C. Watts, R. F. Gandy, P. E. Phillips, G. Cima, R. Chatterjee, A. Blair, A. Hubbard, C. W. Domier, and Jr. N. C. Luhmann. High resolution electron cyclotron emission temperature profile and fluctuation diagnostic for Alcator C-Mod. *Rev. Sci. Instrum.*, 70(1):1011–1013, 1999.
- [9] B. Coppi, H. P. Furth, M. N. Rosenbluth, and R. Z. Sagdeev. Drift instability due to impurity ions. *Phys. Rev. Lett.*, 17(7):377–379, Aug 1966.
- [10] T. Zhou and B. Coppi. Heavy particle mode as the signature of the I-regime. In *52nd Annual Division of Plasma Physics APS meeting, Chicago, IL, USA*, page TP9.104, 2010.
- [11] T. Ma, B. Coppi, T. Golfopoulos, and T. Zhou. Heavy particle mode: I-regime, magnetic fluctuations and toroidal geometry effects. In *52nd Annual Division of Plasma Physics APS meeting, Chicago, IL, USA*, page TP9.103, 2010.
- [12] B. Coppi. Heavy Particle Modes and Signature of the I-Regime. Submitted to *Physics Letters A*, 2011.
- [13] I. H. Hutchinson. *Principles of Plasma Diagnostics, 2nd Ed.* Cambridge University Press, 2002.
- [14] R. Chatterjee, P.E. Phillips, J. Heard, C. Watts, R. Gandy, and A. Hubbard. High resolution ECE radiometer for electron temperature profile and fluctuation measurements on Alcator C-Mod. *Fusion Engineering and Design*, 53:113–121, 2001.
- [15] C. Watts, H. J. Hartfuss, and M. Haese. Comparison of different methods of electron cyclotron emission-correlation radiometry for the measurement of temperature fluctuations in the plasma core. *Review of Scientific Instruments*, 75:3177–3184, 2004.
- [16] V. S. Udintsev, M. Goniche, J. L. Segui, G. Giruzzi, D. Molina, F. Turco, G. T. A. Huysman,

- P. Maget, and Tore Supra Team. *Fusion Science and Technology*, 50:508, 2006.
- [17] G. Cima, R. V. Bravenec, A. J. Wootton, T. D. Rempel, R. F. Gandy, C. Watts, and M. Kwon. Core temperature fluctuations and related heat transport in the Texas Experimental Tokamak-Upgrade. *Physics of Plasmas*, 2(3):720–726, 1995.
- [18] C. Watts. *Fusion Sci. & Technol.*, 52:176, 2007.
- [19] A. E. White, L. Schmitz, G. R. McKee, C. Holland, W. A. Peebles, T. A. Carter, M. W. Shafer, M. E. Austin, K. H. Burrell, J. Candy, J. C. DeBoo, E. J. Doyle, M. A. Makowski, R. Prater, T. L. Rhodes, G. M. Staebler, G. R. Tynan, R. E. Waltz, and G. Wang. Measurements of core electron temperature and density fluctuations in DIII-D and comparison to nonlinear gyrokinetic simulations. *Phys. Plasmas*, 15:056116, 2008.
- [20] L. Schmitz, A. E. White, T. A. Carter, W. A. Peebles, T. L. Rhodes, K. H. Burrell, W. Solomon, and G. M. Staebler. Observation of reduced electron-temperature fluctuations in the core of H-mode plasmas. *Phys. Rev. Letters*, 100:035002, 2008.
- [21] J. S. Bendat and A. G. Piersol. *Random Data*. John Wiley and Sons, NY, 2000.
- [22] M. Bornatici, F. Engelmann, S Novak, and V Petrillo. Absorption of a plasma of finite density around the electron cyclotron harmonics. *Plasma Physics*, 23(12):1127, 1981.
- [23] D.V.Bartlett, A.E. Costley, L.Porte, R.Prentice, N.A.Simon, and G. Sips. Measurement of electron temperature and density of the edge plasma of JET by ECE and microwave reflectometry. *Journal of Nuclear Materials*, 176 and 177:1064–1069, 1990.
- [24] A.E.Hubbard, R. L. Boivin, R. S. Granetz, M. Greenwald, I. H. Hutchinson, J. H. Irby, Y. In, J. Kesner, B. LaBombard, Y. Lin, J. E. Rice, T. Sunn Pedersen, J. A. Snipes, P. C. Stek, Y. Takase, S. M. Wolfe, and S. Wukitch. Measurements of the high confinement mode pedestal region on Alcator C-Mod. *Phys. Plasmas*, 5(5):1744, 1998.
- [25] L Barrera, E de la Luna, L Figini, M N A Beurskens, M Brix, F Castejn, P C de Vries, D Farina, M Kempenaars, P Lomas, J Mailloux, I Nunes, E R Solano, and JET-EFDA Contributors. Inboard and outboard electron temperature profile measurements in JET using ECE diagnostics. *Plasma Physics and Controlled Fusion*, 52(8):085010, 2010.
- [26] J. W. Hughes, D. Mossessian, K. Zhurovich, M. DeMaria, K. Jensen, and A. Hubbard. Thomson scattering upgrades on Alcator C-Mod. *Review of Scientific Instruments*, 74(3):1667–1670, 2003.
- [27] I. G. J. Classen, J. E. Boom, W. Suttrop, E. Schmid, B. Tobias, C. W. Domier, Jr. N. C. Luhmann, A. J. H. Donné, R. J. E. Jaspers, P. C. de Vries, H. K. Park, T. Munsat, M. García-Muñoz, and P. A. Schneider. 2D electron cyclotron emission imaging at ASDEX upgrade (invited). *Review of Scientific Instruments*, 81(10):10D929, 2010.
- [28] T. D. Rempel, R. F. Gandy, and A. J. Wootton. Density fluctuation effects on electron cyclotron emission correlation measurements in optically gray plasmas. *Rev. Sci. Instrum.*, 65:2044, 1994.
- [29] S. Sattler, H. J. Hartfuss, and W7-AS Team. Experimental evidence for electron temperature fluctuations in the core plasma of the W7-AS stellarator. *Physical Review Letters*, 72:653, 1994.
- [30] H. J. Hartfuss, S. Sattler, and W7-AS-Team. Electron temperature fluctuation measurements on the W7-AS stellarator. *Proc. 9th Joint Workshop on ECE and ECRH (Borrego Springs, USA, 1995) ed. J. LOHR (World Scientific, Singapore, 1995)*, page 369, 1995.
- [31] R.J. Groebner, D.R. Baker, K.H. Burrell, T.N. Carlstrom, J.R. Ferron, P. Gohil, L.L. Lao, T.H. Osborne, D.M. Thomas, W.P. West, J.A. Boedo, R.A. Moyer, G.R. McKee, R.D. Deranian, E.J. Doyle, C.L. Rettig, T.L. Rhodes, and J.C. Rost. Progress in quantifying the edge physics of the H-mode regime in DIII-D. *Nuclear Fusion*, 41(12):1789, 2001.
- [32] A. E. White, N. T. Howard, D. R. Mikkelsen, M. Greenwald, J. Candy, and R. Waltz. submitted to PPCF *Plasma Phys. Cont. Fusion*, 00:100100, 2011.
- [33] J A Snipes, B LaBombard, M Greenwald, I H Hutchinson, J Irby, Y Lin, A Mazurenko, and M Porkolab. The quasi-coherent signature of enhanced D- α H-mode in Alcator C-Mod. *Plasma Physics and Controlled Fusion*, 43(4):L23, 2001.
- [34] A. E. Hubbard, R. L. Boivin, R. S. Granetz, M. Greenwald, J. W. Hughes, I. H. Hutchinson, J. Irby, B. LaBombard, Y. Lin, E. S. Marmor, A. Mazurenko, D. Mossessian, E. Nelson-Melby,

- M. Porkolab, J. A. Snipes, J. Terry, S. Wolfe, S. Wukitch, B. A. Carreras, V. Klein, and T. Sunn Pedersen. Pedestal profiles and fluctuations in C-Mod enhanced D-alpha H-modes *Physics of Plasmas*, 8(5):2033–2040, 2001.
- [35] A. G. Lynn, P. E. Phillips, and A. Hubbard. Electron cyclotron emission as a density fluctuation diagnostic. *Rev. Sci. Instrum.*, 75:3859, 2004.
- [36] A. E. White, L. Schmitz, W. A. Peebles, T. A. Carter, T. L. Rhodes, E. J. Doyle, P. A. Gourdain, J. C. Hillesheim, G. Wang, C. Holland, G. R. Tynan, M. E. Austin, G. R. McKee, M. W. Shafer, K. H. Burrell, J. Candy, J. C. DeBoo, R. Prater, G. M. Staebler, R. E. Waltz, and M. A. Makowski. A correlation electron cyclotron emission diagnostic and the importance of multifield fluctuation measurements for testing nonlinear gyrokinetic turbulence simulations. *Review of Scientific Instruments*, 79(10):103505, 2008.
- [37] A. E. White, W. A. Peebles, T. L. Rhodes, C. H. Holland, G. Wang, L. Schmitz, T. A. Carter, J. C. Hillesheim, E. J. Doyle, L. Zeng, G. R. McKee, G. M. Staebler, R. E. Waltz, J. C. DeBoo, C. C. Petty, and K. H. Burrell. Measurements of the cross-phase angle between density and electron temperature fluctuations and comparison with gyrokinetic simulations. *Physics of Plasmas*, 17(5):056103, 2010.

Figures

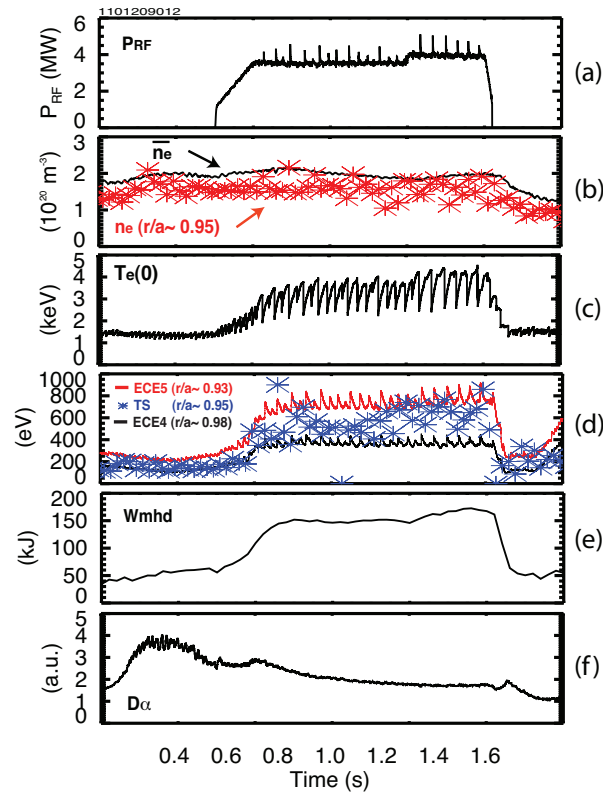


Figure 1. (Colour online) Plasma parameters from Alcator C-Mod discharge 1101209012, showing the input RF-power and the increase in core temperature, edge temperature, and stored energy that occur during the I-mode phase ($0.8 < t < 1.5$ sec). Across the L-I transition ($t_{LI} \approx 0.75$ sec), there is little to no change in line averaged density and edge density. (a) RF power; (b) line averaged density (black-solid) and edge density (red symbols); (c) central temperature $T_e(0)$; (d) edge temperature T_e , measured with Thomson Scattering, $r/a \sim 0.95$, (blue symbols) and measured with the fast ECE radiometer, channel 4 at $r/a \sim 0.98$ (black solid) and channel 5 at $r/a \sim 0.93$ (red solid); (e) stored energy; (f) edge D- α emission.

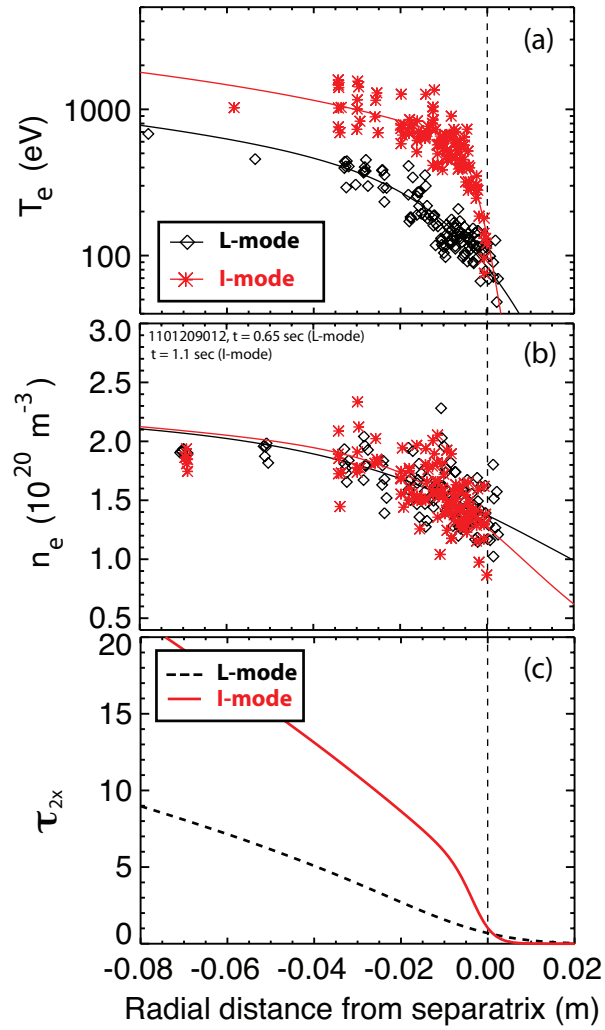


Figure 2. (Colour online)(a) Profiles of edge electron temperature and (b) density are shown for the L-mode (black-triangles) phase and the I-mode phase (red-asterisk) of discharge 1101209012. Thomson scattering and ECE data are fit with a modified tanh function. Density profiles remain similar in L-mode and I-mode, but there is significant increase in edge temperature and the formation of a clear edge temperature pedestal in I-mode. (c) The optical depth is much higher in I-mode ($\tau > 4$) just ~ 5 mm inside the separatrix compared to L-mode ($\tau \approx 1$), which allows for clear measurements of electron temperature with edge radiometer channels.

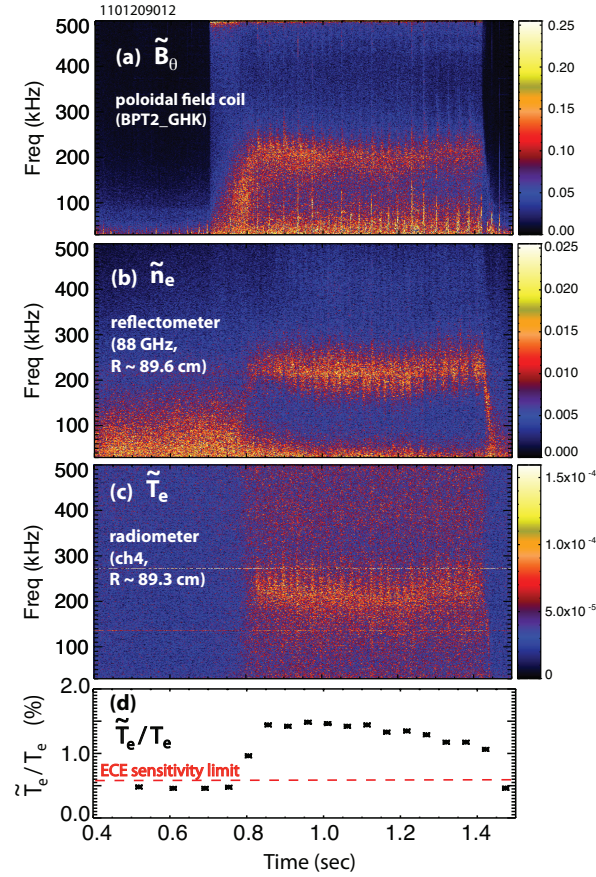


Figure 3. (Colour online) Contours of time-resolved autopower spectra from edge fluctuations showing typical WCM features during I-mode ($0.8 < t < 1.5$) (a) Autopower spectrum of an edge poloidal magnetic field probe (b) Autopower spectrum of an edge reflectometer signal ($f_{o-mode} = 88$ GHz, $R = 89.6$ cm). (c) Autopower spectrum of edge ECE radiometer channel 4 ($f_{ece} = 241.8$ GHz, $R = 89.3$ cm). (d) Temperature fluctuation level, \tilde{T}_e/T_e (%), in time at the edge of the plasma, calculated from the radiometer channel 4. The sensitivity limit is shown as the red dashed line.

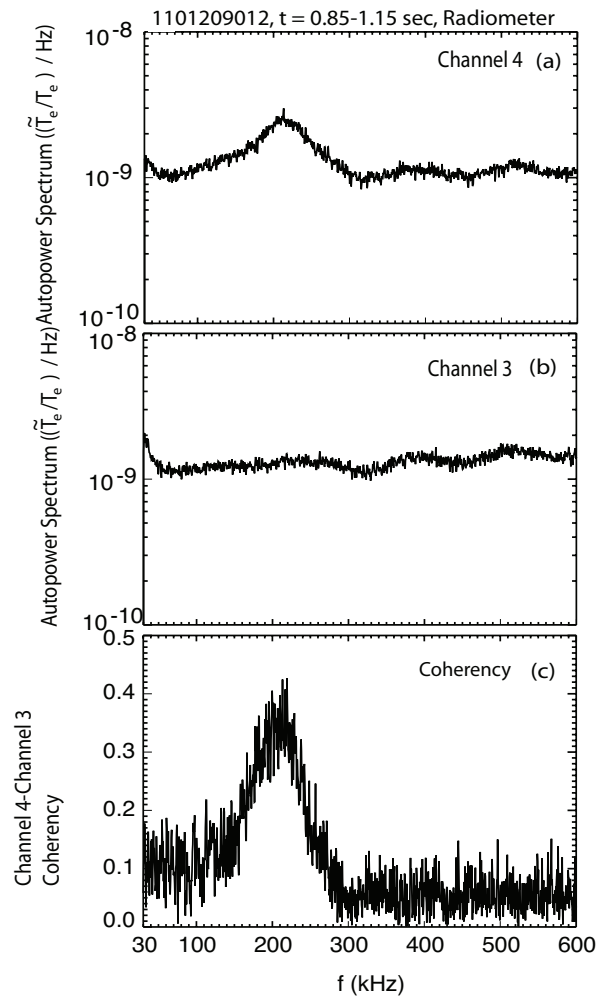


Figure 4. (a) Autopower spectrum of radiometer channel 4 ($r/a \approx 0.98$) showing the WCM. (b) Autopower spectrum of radiometer channel 3 ($r/a \approx 1.00$). The WCM fluctuation level is below the single channel sensitivity at this radius. (c) Coherence spectrum between radiometer channels 3 and 4, showing the WCM correlated on the two channels.

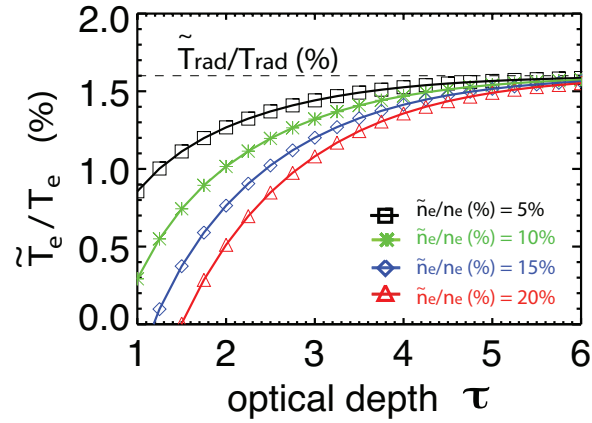


Figure 5. (Colour online) Modeled values of \tilde{T}_e/T_e with density fluctuation levels of $\tilde{n}_e/n_e = 5\%$ (black, squares), 10% (green, asterisks), $\tilde{n}_e/n_e = 15\%$ (blue, diamonds) and 20% (red, triangles) plotted versus optical depth, τ . The horizontal dashed line labels the measured fluctuation level, $\tilde{T}_m/T_m = 1.6\%$. For optical depths above $\tau = 4.5$, $\tilde{T}_e/T_e \approx \tilde{T}_m/T_m$, showing that density fluctuations do not contribute to the measured fluctuation level.